Simple and low-cost compliant leg-foot system

Friedrich Meyer, Alexander Spröwitz
Department of Mechatronics
Technische Universität Ilmenau
Ilmenau, Germany
{friedrich.meyer,alexander.sproewitz}@stud.tu-ilmenau.de

Max Lungarella, Luc Berthouze
Neuroscience Research Institute
Tsukuba AIST Central 2
305-8568 Tsukuba, Japan
{max.lungarella,luc.berthouze}@aist.go.jp

Abstract—We present the design of a simple and low-cost humanoid leg-foot system featuring compliant joints and springy feet. The mechanical compliance of the individual joints can be adjusted by means of visco-elastic material, or metal. To explore some of the relevant characteristics of the proposed system, we performed a series of experiments in which the leg was dropped from a fixed height. Combinations of different materials in the joints (silicone rubber, latex, and brass) as well as a rigid or a compliant foot were used. Additional data were obtained through of a Lagrangian analysis of the leg-foot system. Our analyses show that compliant joints not only reduce impactive forces, but also induce smoother joint trajectories. Further, by employing a compliant foot, a higher energy efficiency for the movement is achieved.

I. INTRODUCTION

Due to the detrimental effects on positional accuracy, stability, and control bandwidth, traditional robot design has striven to maximize the impedance between actuator and load, and to minimize joint compliance [3], [12]. Generally speaking, compliance represents one of the main problems for traditional control paradigms, because it introduces uncontrollable and underactuated degrees of freedom. Modern control theory can deal with the presence of such nonactuated degrees of freedom, but a combination of rather sophisticated nonlinear control strategies and analytical methods for modeling flexible body dynamics has to be employed. Hence the need for high impedance actuation mechanisms and high stiffness materials (e.g. metals).

Mechanically compliant systems (biological and artificial) have, however, advantages as well:

- lower inertial forces in the case of compliant joints, and lower reflected impedance in the case of compliant actuators;
- potential for efficient (elastic) energy storage and restitution [1];
- instantaneous dynamical compensating for the destabilizing effects that result from transmission delays and controller lag in (neural) feedback control [6];
- greater shock tolerance and reduced damage in case of accidental collisions due to the low-pass filter properties of compliant/elastic elements (of crucial importance if robots have to interact with humans, for instance).

It is therefore not surprising that several robots with compliant actuators, flexible links or compliant joints have been designed. Most notable is the series elastic actuator developed by Pratt and Williamson [8], which was used in the robots COG [14], and in Spring Flamingo [10]. Series elastic actuators are actuators capable of actively controlling their compliance that have an elastic element (typically a spring) in series with the output of the actuator (motor and gear-box). A sensor measures the deflection of the elastic element from its resting position, and the force acting on it is implied by Hooke's Law (stating that the force is proportional to the deflection). In short, series elastic actuators provide more accurate and stable force control, shock tolerance, and low impedance actuation. Other successful robots employ also compliance in one form or another. The Honda humanoid robot P2, for instance, has force/torque sensors located in the springy feet and controls the joint trajectories in order for the foot to comply with the ground [5]. Its springy rubber feet are an instance of passive compliant mechanism.

Our long-term goal is to build a compliant robot leg-foot system that will be used to perform systematic jumping experiments inspired by a study on infants by Goldfield et al. [4]. Obviously such a system needs to be lightweight and robust enough to cope with the dynamic loads of jumping. Merely employing powerful actuators, and rigidly connected parts for hip, thigh, shank, and foot, however, would not provide us with an appropriate robotic system for exploiting such a task. Rigid connected parts are unable to absorb sudden impact loads passively.

In this article, we first present the design of a leg featuring compliant joints and a compliant foot with toes. Then describe the real and the simulated robotic system built to test the leg. The results are exposed in Section V, and discussed in Section VI. Eventually, we conclude and point to some future work.

II. COMPLIANT LEG-FOOT SYSTEM

The compliant "core" of the joints were fan-shaped elastomer springs (or wedges) made either of silicone rubber, or latex. This particular form was chosen so as to avoid torsional forces on the elastomer. To get a stiff joint we inserted a brass-wedge. The springs were 6 mm in thickness, had an outer radius of 12.5 mm, and formed an angle of 120°. We varied their shape, using full springs, springs with holes, and springs with a neck on the outer rim (see Fig. 1). For the experiments described in Section V,

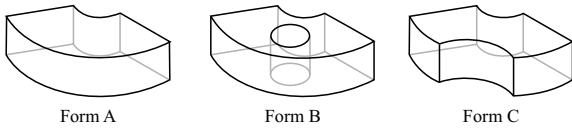we used full springs (Form A) of brass, latex, and silicone rubber.

Fig. 1. Various shapes of springs. Form A: full spring, Form B: spring with whole; Form C: spring with neck on the outer rim.

To simplify the mounting and unmounting of the springs, they were placed inside closed brass bushes (Fig. 2). This allowed us to easily test different types of springs without having to modify the mechanical setup of the system. The bush itself consisted of two circular brass wedges used to compress the springs. These two parts were 6 mm in thickness (like the springs), with an angle of 120° (see Fig. 2). One of these parts was screwed to the bush, the other one to the lid.

The insertion of the spring between the two identical brass parts resulted in an asymmetric compliant joint: Compliant in one direction of movement, and stiff in the other. That is, by compressing the elastomer the bush behaved like a nonlinear torsion spring, whereas by having the two brass parts press against each other, the system was stiff.

This asymmetry of the joint was particularly useful for modeling the characteristic movement limitation of human knee joints (i.e., hard stop of the rotation of the knee joint).
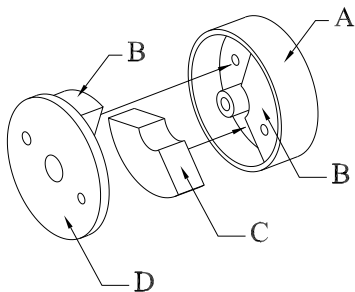

Fig. 2. Schematic representation of the joint, exploded view. (A) bush; (B) fan-shaped brass-wedge used to compress the springs; (C) spring; (D) lid. Depending on the direction of rotation the line of force goes from brass-wedge to brass-wedge (B-to-B), or from brass-wedge over the spring to the other brass-wedge (B-over-C-to-B).

A note on the choice of the employed springs. Because spring systems found in biological systems are highly non-linear, it seemed inappropriate to use linear springs, such as helical or torsional springs. Silicone rubber and latex, on the other hand, are elastomers displaying a nonlinear relationship between applied force and resulting compression. We estimated the force-compression relationship of our springs, by applying force to the compliant joint and measuring the resulting angular displacement. We then fitted the obtained angle-force curve via regression to a power function, which was subsequently used to simulate the compliant joint.

A significant disadvantage of elastomer-based springs is their plastic deformation when subject to stress for a longer period of time. This deformation was higher in the silicone than in the latex spring. In addition to the compliant joints, we constructed a compliant foot consisting of a rigid heel and two spring-metallic toes, which was inspired by the human foot.
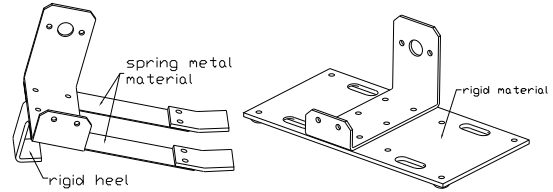

Fig. 3. (Left) compliant foot. (Right) rigid foot.

III. EXPERIMENTAL SETUP

To the test our leg-foot system we built a two legged robot with an overall weight of 1.3 kg. Actuation of hip, knee, and ankle joints was provided by six high-torque RC servo motors (Hitec HS-945MG). The motor position commands were generated on a PC, and then sent via the serial interface to a PIC16F877 responsible for the low-level control of the motors.
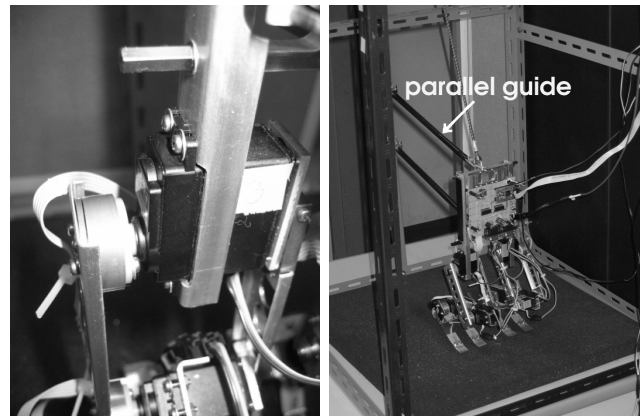

Fig. 4. (Left) bush serially connected to servo motor and shank. (Right) side-view of our experimental setup.

The motors were mounted onto the individual links of the legs (thigh, shank, and foot), and their axes were attached in series to the spring system. The bush itself was screwed to the plastic horn of the servo motor, and the lid to the actuated part of the leg, that is, hip, knee, or ankle joint, respectively (see Fig. 4 left).

The whole system was intended to stand repeated high impact forces arising while jumping. For this specific movement, the torques and forces are always pointing in the same direction. This means that if the leg structure is falling down and jumping up again, the torque in all joints has the same direction for both parts of the movement. The way we constructed the joints allowed us to neglect the elastic reaction in the joints in one direction (see Fig. 2).

IV. Experiments

A. Real robotic system, dropping experiment

For the drop experiments, we mounted the robots back to a parallel guide to increase the reproducibility of the experiment (see Fig. 4 right).

At the outset of each experiment, the knee and ankle joints were set to approximately 90°, and the hip joint was set to 45° (see Fig. 5). We used three types of joints, a stiff one (made of brass), and two compliant ones (made of silicone or latex), and two types of foot shapes: rigid and flat, or compliant with two copper toes (Fig. 3). Drop experiments were performed with the six possible permutations of these parameters. In addition, these experiments were performed with a tension spring on top of the robot (to see the difference by increasing the springiness of the system). The movements of the joints relative to a fixed frame of reference were measured by tracking colored markers placed on the robot's hip, knee, and ankle. The tracking system's temporal resolution was 33 msec, and its spatial resolution approximately 1 cm. The dropping height was approximately 36 cm (measured from the hip). Please note that in this experiment the motors were blocked.

B. Simulation

In parallel to the mechanical construction, we performed a simulation of the robotic system. To have a closer look at the forces acting in the joints we neglected the deformation of the metal parts. Thus, we performed a Lagrangian analysis, and not a finite element methods (FEM) analysis. The calculation itself was done with ALASKA (Advanced LAgrangian Solver in Kinetic Analysis) [2].

We made some simplifying assumptions. First, all elements of the robot that did not move relative to each other were considered to be one single part. This assumption is valid, if the new element has the same mass and moments of inertia as the assembly of the real parts. Second, we limited the simulation to only one side of the robot, that is, whereas the real robot had two legs, we simulated only one leg and one part of the hip. This simplification is valid, as long as the left and right side of the real robot are controlled in the same way. As a result, the whole system consisted of four main elements: hip, thigh, shank and foot (A, B, C and D in Fig. 5). To stabilize the system, the back of the robot was fixed to a parallel guide, such as the one used in the real setup.

We constructed two types of feet. One was a rigid square plate contacting the ground in four points, the other one used two flexible toes and a rigid heel with totally three contact points. While the springiness of the toes could be measured and implemented in the simulation, the damping was adjusted by comparing the simulation output to the measurement (see Sec. V).

The impact forces on ground contact and inside the bushes were simulated as imposed forces of a spring-damping complex when below the joint angle was below a threshold.

In order to simulate the rubber springs, we used a low damping, which was adapted by comparison of the output values, and a measured springiness. The principle for the force calculation was the same as used for the ground and bush reaction.

The simulation setup was: an angle of 14.3° of the parallel guide, which resulted in a height of approximately 23 cm of the foot over ground, depending on the angles of the joints. These were prebent in an angle of approximately 45° in the hip and approximately 90° in knee and foot. A fine adjustment of the angles was necessary, because it was impossible to give accurate angles in the joints for the real setup due to backlash.

For the integration a Runge-Kutta integration algorithm with fixed timestep was used. The stepwidth was 0.01 milliseconds. Longer timesteps resulted in an exceedance of energy at the moment of impact. The usage of integration algorithms with variable stepwidth (Shampine-Gordon, Lsode for stiff/nonstiff joints, Dormand-Prince Order 5/8) resulted in an exceedance of either input variables or calculation time at the moment of ground contact.

C. Repetitive kick experiment

For this experiment, only one leg was used. The leg was fixed so as to be able to move freely. The knee and the ankle joints were stiff (brass-wedge), whereas the hip joint's compliance was systematically varied. The hip motor was actuated and moved the stiff leg from the back to the front, and back, with a frequency of approximately 0.6 Hz. Due to the aforementioned asymmetry, the frontal leg swing (falling edge in the graphs of Fig. 9), was without compliance (force was directly propagate from the lid wedge to the bush wedge). In contrast, the backward movement used the material between the two fixed wedges.

V. Results

A. Dropping experiment

One result of this experiment was that in a system with compliant foot, the oscillations were more pronounced than in a system with a rigid foot (see also Fig. 8). By attaching a spring on top of the robot the amplitude of the oscillations increased (in all cases). What is further evident is the high damping achieved with compliant joints compared to the one for non-compliant joints. The damping was higher for springs made out of silicone rubber than for latex springs.

B. Simulation

The springs in the joints were simulated by means of a spring-damping system. Because this does not exactly match the visco-elastic force feedback of an elastomer, the damping had to be adjusted for the individual setups. Due to backlash in the joints of the real system, it was not possible to measure the exact initial angles. Hence, we had to fine tune them as well. The resulting match between simulated trajectories and the real ones can be seen in Fig. 6.

There was a problem of time shift in the fixed joints on impact. The curves are identical for the free fall and
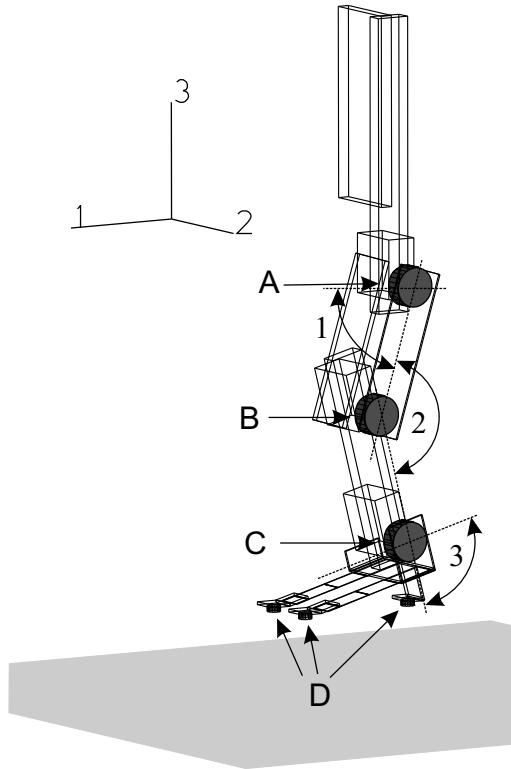
Fig. 5. Schematic representation of the simulated setup. The markers on hip (A), knee (B), ankle (C), and ground contact points (D) have the same position as the ones used on the real robot. The angles 1, 2, and 3 represent the hip, knee, and ankle joint angles, respectively.
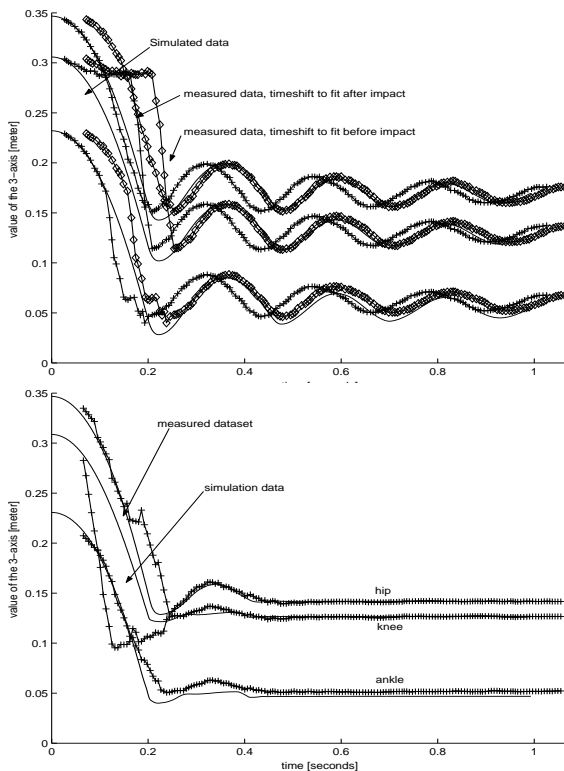

Fig. 6. (Top) Displacement of the ankle, knee, and hip joints along the 3-axis for stiff joints (in meter). (Bottom) Displacement of the ankle, knee, and hip joints along the 3-axis for compliant joints with Latex-springs (in meter). The data of real and simulated setup are overlapped. The unit of the horizontal axis is seconds.

for the time after the first impact, but vary in the time of impact. We were not able to figure out the reason for this mismatch so far. Apart from that, the output of the simulation reproduces well what we observed in the real setup (the trajectories are almost identical). Because the movements of the single parts as well as of the masses and moments of inertia of the system were the identical for both simulation and real setup, it is thus justified to consider the forces in both setup as identical.

As can be seen from Fig. 7, the torques in all joints are high on the first impact, but the system with the compliant joints has no further peaks due to its high damping. As mentioned above, the springiness is imposed when above a threshold. This results in the high frequency noise that can be seen especially in the knee at the end of the simulation. This does not occur in a real setup. There is a small force swinging after the first and second impact that can be seen on the fixed joints. This is because of the toes, which are free swinging after lift-off. Because of the low sampling rate of the camera in the real setup this could not be seen. Please note that the peaks on the flexible system do not occur on impact time due to the backlash within the bushes.
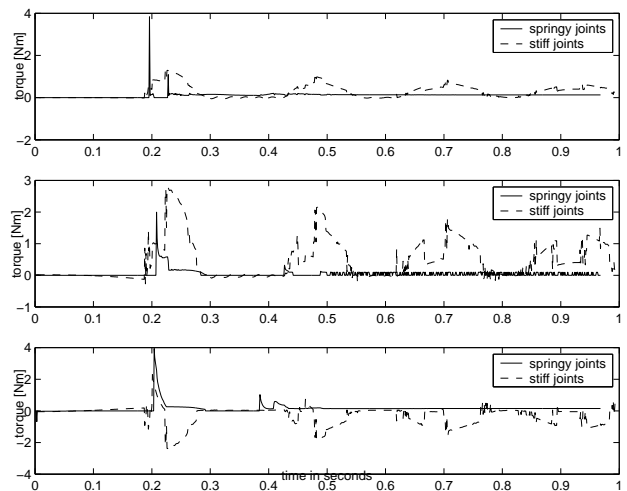

Fig. 7. Torques (in Nm) in the joints of the simulated setup. A positive torque is the result of a force that points in the direction of the springy part, whereas for a negative torque the resulting force points in the direction of the brass-wedge.

In contrast to the stiff system, the torques in the compliant system are only in one direction. Thus, when the task for the system is to jump or drop, it is possible to concentrate on the compensation of impact peaks in only one direction, that obviously simplifies the setup.

C. Repetitive kick experiment

The results of this experiment are presented in Fig. 9. First, the angular displacement from the resting position of the leg ($\pi/2$ rad), represented by the longer horizontal part of the graphs, is biggest for brass (0.78 rad). Smaller than brass is the one for latex (0.58 rad); the smallest being the one of silicone (0.41 rad). This angular displacement is a clear indication of the softness of the materials used in the
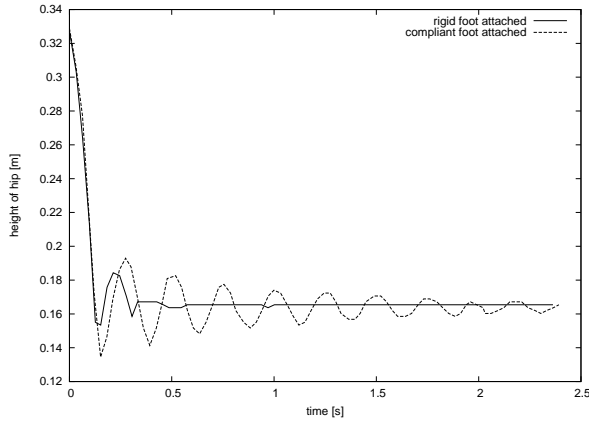
Fig. 8. Vertical displacement of hip for real robot dropped from a height of 36 cm. The amplitude of the first rebounce shows the higher storage of energy by the compliant foot compared to the rigid one.

joints. The softer the material, the more gravity can affect the angle by pushing the leg into the springs.

As explained above, the down-going edge of the graphs represent the forward kick of the leg, the up-going edge the backward kick. The damping of the compliant joint appears as a second peak after the main peak, in the top figure (brass material used in the joint). Because after the maximum the leg is not actuated any more, every following movement is representing the passive response due to the inertia of the leg. The brass wedge obviously is not absorbing this energy.

Third, the end position did not change significantly over 300 seconds (190 oscillations of the leg) for all the used wedges (latex, silicone, and brass). Therefore no change of the material properties occurred by stressing the compliant springs with a repeated constant force usually applied on them.

VI. DISCUSSION

Some issues relating to the simulation and the measurements are discussed in this section.

First, in the simulation hard impacts were implemented as spring-damping compounds. This implementation led to high-frequent impacts on the ground and in the bushes, whereas in the real world there is only one contact. This can be seen in the resulting forces in the ground contact points (not displayed here).

Second, the drop experiments were recorded by a tracking system at a framerate of 30 frames per second. Alas, such temporal resolution was not high enough in the case of high impact forces.

Third, while the force in the ankle showed a peak on the first impact of the foot on the floor – shifted by the time necessary to overcome the backlash – the knee did not show any reaction force upon impact. The knee only reacted on the rebouncing in the opposite way shortly after. The result of our simulations show that under a specific angle of attack of the foot at impact time, the knee's springiness was not affected. That is, the movement of the knee remained beneath the threshold given by the backlash
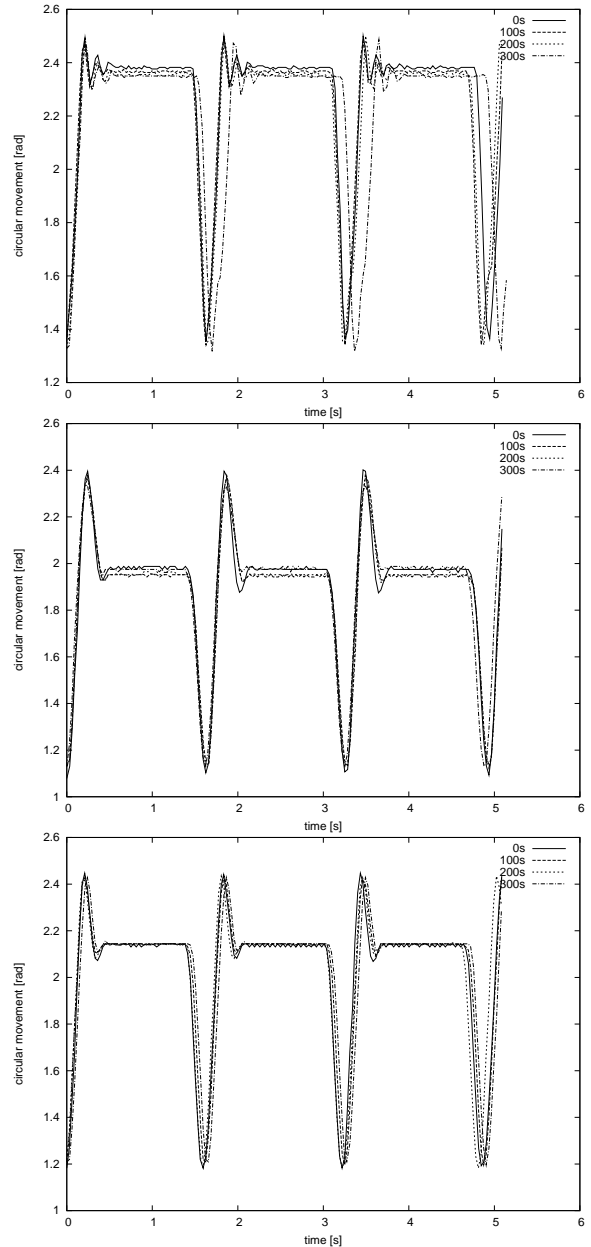

Fig. 9. Angular displacement of the knee joint in response to a repetitive step input of period 1.6 sec to the hip joint. The graphs are overlapped 5.5 sec-snapshots taken at different instants of time (0 sec, 100 sec, 200 sec, 300 sec). (Top) brass spring. (Center) silicone rubber spring. (Bottom) latex spring. Compliant joints are characterized by a larger overshoot (which translates into backlash), and a stronger damping.

for the spring in it. On the other hand, the hip showed a reaction. Since the system was stable at the down position, it seems that the forces in ankle and hip are enough to hold the system. This is obvious, if the system – after impact – is not seen as a closed kinematic loop. In this, the geometrical constrains of the system do not necessarily need a force in all joints to give the structure a specific shape.

A comparison of different output characteristics with different shapes showed that a primary pattern can be recognized and is repeatable, when the same impact angle of the toes is given. If this is the case, changing the overall angles of all three joints results in a change of the 3-values

of the single joints, which are shifted by a constant value. The movement pattern itself remains the same.

There was a problem in the dropping experiment, when all the joints were stiff and the rigid foot was used. The real setup was damaged on impact due to high impactive forces. This problem could be avoided by using a flexible foot. The drawback of this solution, however, was the introduction of oscillations in the system, which made a variable movement speed difficult due to phase coupling. Introducing flexible joints had two advantages. First, the high damping cut off swinging after one phase. Because of this, literally every movement would be possible neglecting the history of the system, i.e., previous movements. Second, multiple jumping using in-phase coupling is possible by usage of the second part of the impact-phase for the next movement. As mentioned above, changing shape and impact-angle changes the characteristics of the curves significantly and predictable. A learning system would by able to adapt to the reaction curves by setting the angles of the joints on impact time and the timing of the next jump phase accordingly.

VII. FUTURE WORK

Eventually, the proposed compliant joint will be part of a system that will be used to perform systematic, potentially time-intensive, jumping experiments. Thus, it will be important to explore the issue of how the spring properties change over time further. Future work will also focus on interfacing the jumping system with a control architecture capable of compensating for the backlash that currently affects the joints. A suitable starting point could be neural oscillators, which driven by touch sensors placed under the feet, and encoders in the joints, could entrain and hence possibly compensate for the backlash.

ACKNOWLEDGMENTS

REFERENCES

[1] Alexander, R.McN. *Elastic Mechanisms in Animal Movement.* Cambridge: Cambridge University Press.

[2] ALASKA (Advanced Lagrangian Solver in Kinetic Analysis) Ver.2.3. Chemnitz Technical University. 1990.

[3] Eppinger, S.D. and Seering,W.P. Three dynamic problems in robot force control. *IEEE Int. Conf. on Robotics and Automation*, pp. 392-397, 1989.

[4] Goldfield, E., Kay, B.A. and Warren, W.H. Infant bouncing: the assembly and tuning of an action system. *Child Development*. vol. 64, pp. 1128-1142, 1993.

[5] Hirai, K., Hirose, M., Haikawa, Y. and Takenaka, T. The development of the Honda humanoid robot. *IEEE Int. Conf. on Robotics and Automation*, pp. 1321-1326, 1998.

[6] Humphrey, D.R. and Reed, D.J. Separate cortical systems for the control of joint movement and joint stiffness: Reciprocal activation and coactivation of antagonist muscles. *Advances in Neurology*, vol. 39, pp. 347-372, 1983.

[7] Lungarella, M. and Berthouze, L. Robot bouncing: on the interaction between body and environmental dynamics. *Proc. of the Workshop on Embodied Cognition*, 2004. (to appear)

[8] Pratt, G.A., Williamson, M., Dillworth,P., Pratt, J., Ulland, K. and Wright, A. Stiffness isn't everything. *4th Proc. of the Int. Symp. on Experimental Robotics*, 1995.

[9] Pratt, G.A. and Williamson, M. Series elastic actuators. *IEEE Int. Conf. on Intelligent Robots and Systems*, pp. 399-406, 1995.

[10] Pratt, J. *Exploiting Inherent Robustness and Natural Dynamics in the Control of Bipedal Walking Robots* Ph.D. Thesis, Computer Science Department, MIT, Cambridge, MA, 2000.

[11] Schimmels, J.M. and Huang, S. A passive mechanism that improves robotic positioning through compliance and constraint *Robotics and Computer-Integrated Manufacturing*, vol. 12(1), pp. 65-71.

[12] Spong, M.W. Modeling and control of elastic joint robots. *Journal of Dynamic Systems, Measurement, and Control* vol. 100, pp. 310-319, 1987.

[13] Sugano, S., Tsuto, S. and Kato, I. Force control of the robot finger joint equipped with mechanical compliance adjuster. *Proc. of the 1992 IEEE/RSJ Int. Conf. on Intelligence Robots and Systems*, pp. 2005-2013.

[14] Williamson, M.M. Neural control of rhythmic arm movements. *Neural Networks*, vol. 11(7/8), pp. 1379-1394, 1998.